OPEN

NPG Asia Materials (2015) 7, e210; doi:10.1038/am.2015.91

www.nature.com/am

ORIGINAL ARTICLE

High thermoelectric performance in copper telluride

Ying He[1,2,3], Tiansong Zhang[2], Xun Shi[1,2], Su-Huai Wei[4] and Lidong Chen[1,2]

Recently, $Cu_{2-\delta}S$ and $Cu_{2-\delta}Se$ were reported to have an ultralow thermal conductivity and high thermoelectric figure of merit *zT*. Thus, as a member of the copper chalcogenide group, $Cu_{2-\delta}Te$ is expected to possess superior *zTs* because Te is less ionic and heavy. However, the *zT* value is low in the Cu_2Te sintered using spark plasma sintering, which is typically used to fabricate high-density bulk samples. In addition, the extra sintering processes may change the samples' compositions as well as their physical properties, especially for Cu_2Te, which has many stable and meta-stable phases as well as weaker ionic bonding between Cu and Te as compared with Cu_2S and Cu_2Se. In this study, high-density Cu_2Te samples were obtained using direct annealing without a sintering process. In the absence of sintering processes, the samples' compositions could be well controlled, leading to substantially reduced carrier concentrations that are close to the optimal value. The electrical transports were optimized, and the thermal conductivity was considerably reduced. The *zT* values were significantly improved—to 1.1 at 1000 K—which is nearly 100% improvement. Furthermore, this method saves substantial time and cost during the sample's growth. The study demonstrates that $Cu_{2-\delta}X$ (X = S, Se and Te) is the only existing system to show high *zTs* in the series of compounds composed of three sequential primary group elements.
NPG Asia Materials (2015) **7,** e210; doi:10.1038/am.2015.91; published online 14 August 2015

INTRODUCTION

Green and renewable energy sources have attracted much attention because of concerns about pollution and limited oil sources. Technology based on thermoelectric (TE) materials is appealing because it can realize direct conversion of waste heat to electric energy. The dimensionless figure of merit (zT) is often used to evaluate the TE performance of a material; a large zT is required to achieve a high energy conversion efficiency. The zT is defined as $S^2\sigma T/\kappa$, where S is the Seebeck coefficient, σ is electrical conductivity, T is absolute temperature and κ is thermal conductivity (consisting of carrier thermal conductivity κ_c and lattice thermal conductivity κ_L).[1–3] Application of TE technology is not widespread because of the limited *zTs*, which results in low conversion efficiency. Improvement of materials' performance is still the key to developing the TE technique. Tuning the electron and phonon transports has greatly enhanced the *zTs* for many types of materials over the past decade.[4–10]

Recently, copper selenide ($Cu_{2-\delta}Se$)[11–15] and copper sulfide ($Cu_{2-\delta}S$)[16,17] with liquid-like characteristics were shown to be excellent TE materials with exceptionally low thermal conductivity and high TE performance. *zTs* as high as 1.5 in $Cu_{2-\delta}Se$ and 1.7 in $Cu_{2-\delta}S$ at 1000 K have been achieved, which are among the top values in bulk TE materials. $Cu_{2-\delta}Te$ belongs to the same group of materials. Because tellurium is heavier than sulfur and selenium, the thermal conductivity in telluride is usually expected to be lower than that in selenide or sulfide. In addition, because tellurium is less electronegative, the chemical bonds for tellurides should be less ionic than those for sulfides and selenides, and the carrier mobility should be large in tellurides. These two features make tellurides potentially important TE materials. In fact, many of the state-of-the-art TE materials are tellurides, such as PbTe,[1,2,5] Bi_2Te_3[18,19] and $AgSbTe_2$.[20] The reported high TE performance in $Cu_{2-\delta}Se$ and $Cu_{2-\delta}S$ indicates that a high *zTs* may also be achieved in $Cu_{2-\delta}Te$. However, recent studies showed that the *zTs* in Cu_2Te is only approximately 0.3 at 900 K,[21,22] which is much lower than those in Cu_2Se and Cu_2S. Historically, the *zTs* in the tellurides have been reported to be higher than those in the selenides or the sulfides in classic TE materials, such as PbX (X = S, Se or Te)[1,2,5,23] and Bi_2X_3 (X = S, Se or Te).[1,2,18] The breakthrough of the *zTs* in $Cu_{2-\delta}X$ (X = S, Se or Te) is highly unusual. By comparing the TE properties of $Cu_{2-\delta}X$, we found that the abnormality is because Cu_2Te has high electrical conductivity and low thermopower as compared with $Cu_{2-\delta}Se$ or $Cu_{2-\delta}S$ owing to its severe copper deficiency. Although the stoichiometric chemical ratio of 2:1 for Cu and Te is used to increase copper levels as much as possible during the sample growth process, the Cu_2Te bulk materials created using spark plasma sintering (SPS)[21]—the same process used for $Cu_{2-\delta}Se$ or $Cu_{2-\delta}S$—still have a marked copper deficiency as well as a low *zTs*.

TE technology is a fully solid-state technique, and its performance is determined primarily by materials' density. A high density approaching a material's theoretical density is typically required in bulk materials for high energy conversion efficiency to optimize the

[1]State Key Laboratory of High Performance Ceramics and Superfine Microstructure, Shanghai Institute of Ceramics, Chinese Academy of Sciences, Shanghai, China; [2]CAS Key Laboratory of Materials for Energy Conversion, Shanghai Institute of Ceramics, Chinese Academy of Sciences, Shanghai, China; [3]University of Chinese Academy of Sciences, Beijing, China and [4]National Renewable Energy Laboratory, Golden, CO, USA
Correspondence: Professor X Shi, State Key Laboratory of High Performance Ceramics and Superfine Microstructure, Shanghai Institute of Ceramics, Chinese Academy of Sciences, 1295 Dingxi Road, Shanghai 200050, China.
E-mail: xshi@mail.sic.ac.cn
Received 28 February 2015; revised 11 June 2015; accepted 21 June 2015

electrical transport properties. Partial covalent bonds and partial ionic bonds are the dominant chemical bonds in most TE materials. However, the atomic diffusion rates are usually low in these materials. SPS, or hot-pressing, is usually used to sinter powder materials to achieve high-density bulk samples; this technique has been used in nearly all bulk TE materials. These materials are different from metals and ceramics, which have high atomic diffusion rates that can be densified using direct annealing without extrinsic pressure (pressureless sintering). However, the extra SPS processes may slightly change the samples' compositions as well as their physical properties. In $Cu_{2-\delta}X$ (X = S, Se, Te), even though S and Se elements have high vapor pressure, the chemical compositions of $Cu_{2-\delta}S$ and $Cu_{2-\delta}Se$ are easier to control than that of Cu_2Te. This may be attributable to the chemical bonds. S/Se is smaller than Te, and the electronegativity difference between S/Se and Cu is larger than that between Te and Cu. Thus, the ionic bonding between Cu and S/Se is stronger than that between Cu and Te, and the self-compensation between the Cu vacancy and the anion vacancy is more efficient in $Cu_{2-x}S/Cu_{2-x}Se$ than in $Cu_{2-x}Te$. In addition, there are many stable and meta-stable phases in Cu_2Te. Because these phases are very similar in structure and energy, a small change during the sample fabricating process, such as SPS sintering, can affect its structures and phases.

In this paper, we report significantly enhanced TE performance in fully densified Cu_2Te bulk materials achieved by annealing samples directly without the hot-pressing or SPS processes that are typically necessary for TE materials. This very simple and direct material synthesis process not only saves substantial material fabrication time but also effectively tunes carrier concentrations to nearly the appropriate value, which is favorable for increased power and decreased electronic thermal conductivity. With this process, we obtained an improved *zTs* above unity in this simple binary compound.

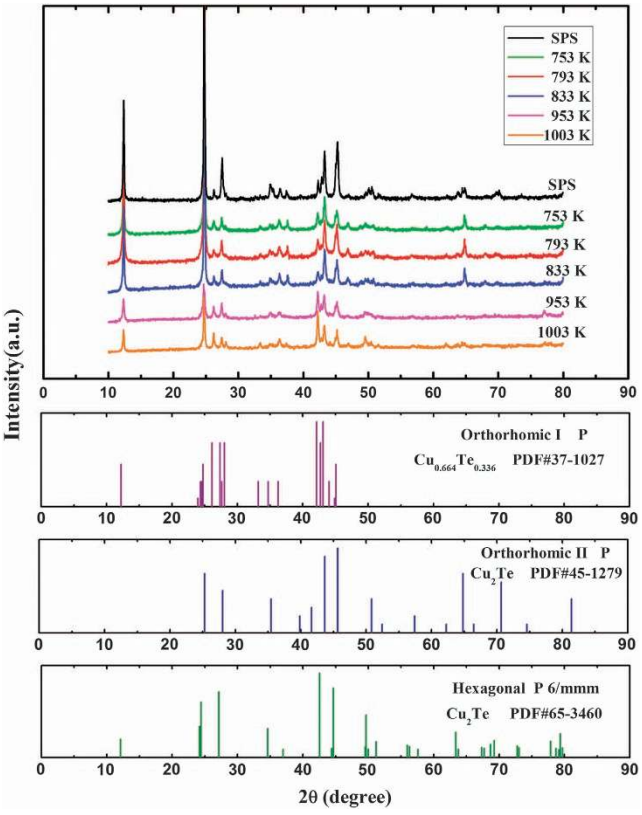

Figure 1 X-ray diffraction patterns of the directly annealed sample as well as the sample sintered using SPS in the Cu_2Te bulk materials. The Cu_2Te samples were directly annealed at 753, 793, 833, 953 and 1003 K. These temperatures were used to mark the samples.

EXPERIMENTAL PROCEDURES

A stoichiometric chemical ratio of 2:1 for Cu (shots, 99.999%, Alfa Aesar, Ward Hill, MA, USA) and Te (pieces, 99.999%, Sigma-Aldrich, St Louis, MO, USA) were weighed out, placed into a graphite crucible and sealed in evacuated silica tubes. The samples were heated to 1393 K over 7 h, maintained at this temperature for 3 h, and then naturally cooled to room temperature. The obtained ingots were ground into powder. Next, the powder was cold-pressed into cylinder pellets and annealed at different temperatures for 7 days. Then, these directly annealed samples were cut into designed pieces for the transport property measurement. One sample, which was annealed at 833 K for 7 days, was removed and crushed into powder, sintered using SPS at 723 K for 5 min and cut into designed pieces to obtain the transport property measurement.

The chemical compositions were measured using energy dispersive spectrometry and inductively coupled plasma-atomic emission spectrometry. The Cu/Te ratio in all the samples was approximately 2, but it is difficult to distinguish subtle differences between phases when the composition deviation is near or lower than the detection limit. The structure was characterized using X-ray diffraction (Cu Kα, D/max-2550 V, Rigaku, Ultima IV, Tokyo, Japan). High-temperature thermopower and electrical resistivity were measured using an Ulvac ZEM-3, Kanagawa, Japan. The thermal conductivity was calculated using the formula $\kappa = D \times C_p \times d$, where D is thermal diffusivity, C_p is heat capacity and d is density. The thermal diffusivity (D) was measured using a laser flash method with a Netzsch LFA457. The specific heat (C_p) data were collected using differential scanning calorimetrics (DSC 404F3, Netzsch, Shanghai, China). No mass was lost after the DSC measurements. The density (d) was measured using the Archimedes method. The Hall resistance (R_H) measurement was performed using the physical property measurement system (PPMS, Quantum Design, San Diego, CA, USA). The hole mobility (μ_H) and carrier concentration (p) were calculated using $\mu_H = \sigma/pe$ and $p = 1/eR_H$, respectively, where e is the elementary charge.

RESULTS AND DISCUSSION

We first used the SPS technique on Cu_2Te to determine its TE properties. The density of the Cu_2Te sintered using SPS is 7.06 g cm^{-3}, which is close to the theoretical density (7.33 g cm^{-3}) based on the hexagonal structure.[24] The room-temperature crystal structure (see Figure 1) for Cu_2Te is very complicated according to the literature, and our X-ray diffraction pattern at room temperature is consistent with the data in Asadov *et al.*[25] The details are discussed below. We measured the TE properties to compare them with the SPS sample described in Ballikaya *et al.*[21] Our sample, as well as those in the literature, showed very large electrical conductivity (approximately a few $10^5\ \Omega^{-1}\ m^{-1}$) and low thermopower (less than 100 μV K^{-1} in the entire temperature range), as indicated in Figure 2. Cu_2Te has a band gap of approximately 1.04 eV.[26] Thus, the ideal chemical stoichiometric ratio compound Cu_2Te should be an intrinsic semiconductor with a very low carrier concentration and electrical conductivity as well as a large thermopower. However, the very high electrical conductivity and low thermopower shown in Figure 2 are quite different from those of the ideal Cu_2Te compound. Because of its extremely high electrical conductivity, the thermal conductivity of Cu_2Te is also quite high, with room-temperature values of approximately 2 W m^{-1} K^{-1} in our sample and above 4 W m^{-1} K^{-1} in the literature[21,22] as compared with that in Cu_2Se (0.98 W m^{-1} K^{-1})[11–15] and Cu_2S (0.36 W m^{-1} K^{-1}).[16] Therefore, the zT in Cu_2Te is much smaller than that in Cu_2Se and Cu_2S, and the best values are only approximately 0.4 at 900 K and 0.55 at 1000 K (see Figure 2). Although we have attempted to tune the synthesis processes to acquire

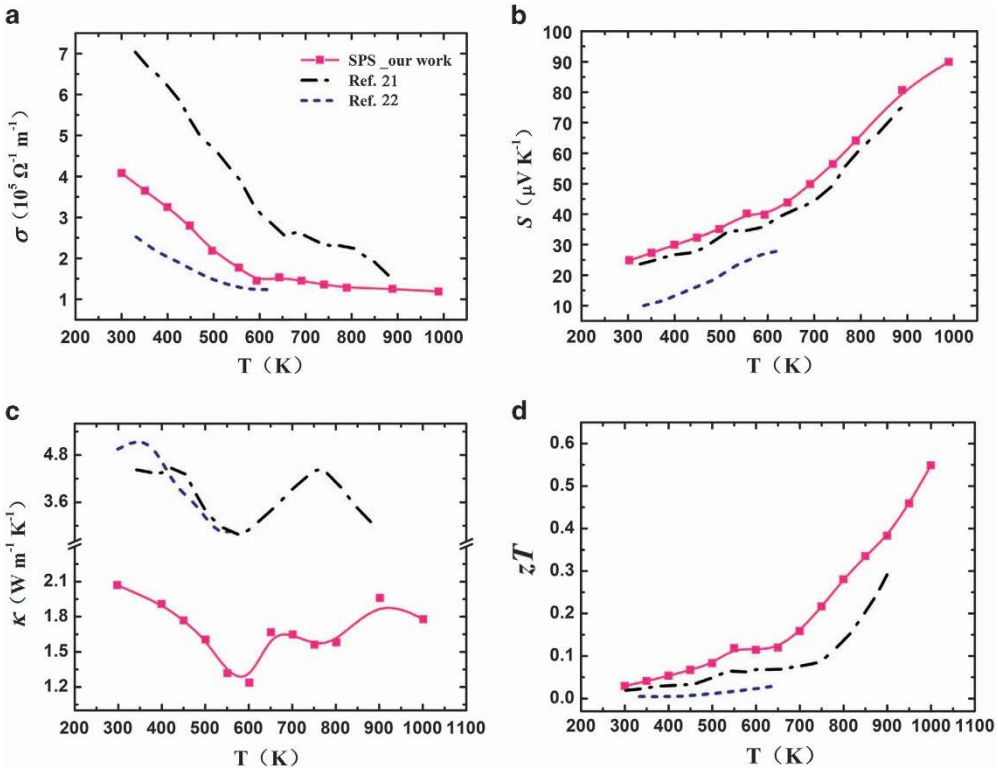

Figure 2 Temperature dependence of the thermoelectric properties of Cu_2Te using spark plasma sintering. (**a**) Electrical conductivity (σ), (**b**) thermopower (S), (**c**) total thermal conductivity (κ) and (**d**) figure of merit (zT). The data from two other studies[21,22] are also shown for comparison.

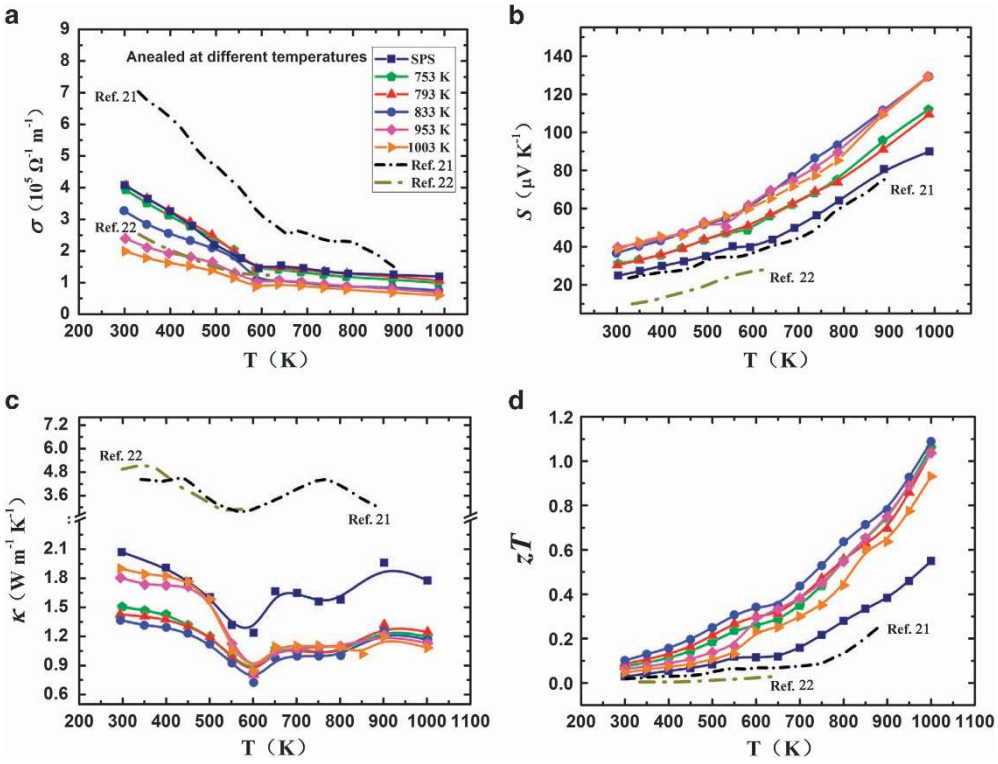

Figure 3 Temperature dependence of the thermoelectric properties of the directly annealed Cu_2Te samples. (**a**) Electrical conductivity (σ), (**b**) thermopower (S), (**c**) total thermal conductivity (κ) and (**d**) figure of merit (zT). The samples sintered using the SPS sample and the Ref-SPS sample are also shown for comparison.

the ideal chemical stoichiometric compositions close to Cu_2Te, we were not successful, and the TE transport properties do not exceed the data shown in Figure 2.

During the sample synthesis process, we found that it was difficult to grind the ingots into a powder. In addition, the Cu_2Te powder can be easily shaped by hand, which seems to be attributable to the partial metallic[27,28] and less ionic chemical bonds in Cu_2Te. Moreover, the calculated formation energy for Cu_2Te is very close to zero,[29] which further demonstrates that the atomic diffusion rates of Cu and Te in the compound should be very high. Similar to metals and ceramics with high atomic diffusion rates but much different from other typical TE materials, high material density can typically be easily achieved in Cu_2Te via direct annealing without extrinsic pressure (pressureless sintering). Thus, we ignored the SPS process and used a direct annealing process to obtain the high-density bulk samples. We placed the powder into a stainless steel cylinder and cold-pressed it into pellets. The pellets were then annealed at the designed temperatures. We first measured the density of these samples using the direct annealing process. It is surprising and interesting that these samples have the same density as that in the sample sintered using SPS, with values ranging from 7.04 to 7.08 $g\,cm^{-3}$.

Figure 1 shows the X-ray diffraction patterns for the samples using direct annealing. Similar to the samples sintered using SPS, all the samples consist of a few mixed structures, which belong primarily to hexagonal and two different types of orthorhombic structures. The SPS sample and those samples directly annealed below 953 K present a better orientation with relatively higher peak densities at low angles (10°–25°). The samples directly annealed at 953 and 1003 K are inclined to be orthorhombic-I dominated structures, with the peak near 65° diminished and the peaks between 40 and 50° enhanced. The structure and phase differences are clearly identified from the heat capacity data in Supplementary Figure S1. These differences may be attributed to the different heat histories, with certain structures being restrained after undergoing extended high-temperature treatment.

We measured the TE properties for all the directly annealed samples from 300 to 1000 K, and the results are presented in Figure 3. The data from the literature and our sample sintered using SPS are also listed for comparison. The discontinuity of the transport properties stems from the phase transitions, with detailed information provided in Supplementary Figure S1. Owing to the intrinsic copper deficiencies in Cu_2Te, all the samples indicate *p*-type conducting in the measured temperature range. It is evident that there was quite a large difference in the transport properties among the samples using different heat treatment conditions and growth processes. The sample sintered using SPS had the highest electrical conductivity and the lowest thermopower. Although the samples using direct annealing had nearly the same temperature dependence as the sample sintered using SPS, their TE properties were very sensitive to the annealing temperatures. The electrical conductivity for the direct annealing samples ranged from approximately 10^5 to $10^4\,\Omega^{-1}\,m^{-1}$, and the thermopower varied between 30 and 130 $\mu V\,K^{-1}$. When the annealing temperature was increased from 753 to 1003 K, the electrical conductivity was reduced and the thermopower was enhanced. The best power factor (*PF*) was near 13 $\mu W\,cm^{-1}\,K^{-2}$, which is more than a 30% enhancement when compared with the sample sintered using SPS. Moreover, the high *PF* in the directly annealed Cu_2Te was the highest among the Cu_2X (X = S, Se and Te) materials[11–17] at high temperatures (see Figure 4). In addition, the thermal conductivity for the directly annealed samples was low owing to the reduced contributions from the charge carriers. Similarly, increasing the annealing temperatures reduced the thermal conductivity from 2 to 1 $W\,m^{-1}\,K^{-1}$. Consequently, the *zT* values were effectively enhanced in the directly annealed samples, with the values exceeding unity at 1000 K. These *zT* values were improved nearly 100% over those of Cu_2Te sintered using SPS or ref-Cu_2Te (see Figure 3d).[21] The fracture morphology and the X-ray diffraction results revealed no clear orientation in our Cu_2Te samples. We tested the electronic transports along two directions (see Supplementary Figure S2). The values were similar in the directions parallel and vertical to the cold-pressing direction, which suggests that the Cu_2Te samples had nearly isotropic transports. We ran the repeatability measurement for our samples, as shown in Supplementary Figure S3. For the sample directly annealed above 1000 K, the data can be fully reproduced. For the samples with a direct annealing temperature below 1000 K, we observed that the data are nearly fully reproduced, except for a minor deviation in some of the samples. This may occur because the measurements do not take a long time and the effect of the additional annealing treatment is not obvious. We therefore recommend that if the directly annealed Cu_2Te samples are applied in practice, they should be annealed at temperatures higher than the working temperatures.

To reveal the origin of the enhanced TE performance in the directly annealed samples, we measured the low-temperature electrical conductivity, carrier concentration and calculated carrier mobility, which are presented in Figure 5. The low-temperature electrical conductivity was decreased when the annealing temperatures were increased in the directly annealed samples, and the sample sintered using SPS had the largest value. This result is the same as the high-temperature data. The samples undergoing additional SPS processes have large carrier concentrations, with values higher than $5\times10^{21}\,cm^{-3}$ in the measurement ranges. The directly annealed samples had much lower carrier concentrations, in the range of 7.4×10^{20} to $1.5\times10^{21}\,cm^{-3}$. The temperature dependence of the carrier mobility was simple in the samples sintered using SPS but complicated in the directly annealed samples (see Figure 5b). The reason is not clear, but it may be linked to the complex mixed crystal structures in the directly annealed samples, as shown in Figure 1. The differences in the mixed phases in the directly annealed samples were supported by the temperature dependence of the electrical conductivity at low temperatures, with the variable-phase transition signals near 150 and 260 K, as shown in Figure 5c and by Bougnot *et al.*[30]

The sound speed of Cu_2Te is 1833 $m\,s^{-1}$,[22] whereas Cu_2S and Cu_2Se have high values of 1991 and 2523 $m\,s^{-1}$, respectively,[16] which indicates that Cu_2Te is softer than Cu_2S and Cu_2Se. Both the soft and ionic bonds reduce carrier mobility. In Cu_2Te, even though it is softer

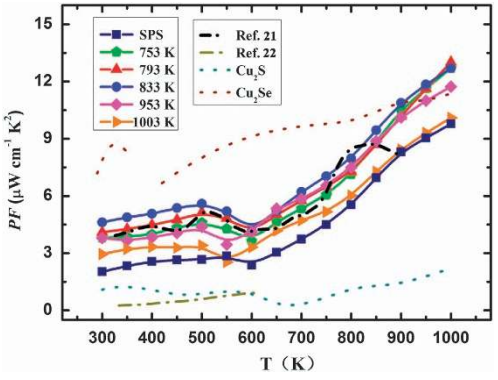

Figure 4 Temperature dependence of the power factors in Cu_2X (X = S, Se or Te).[11,16,21,22]

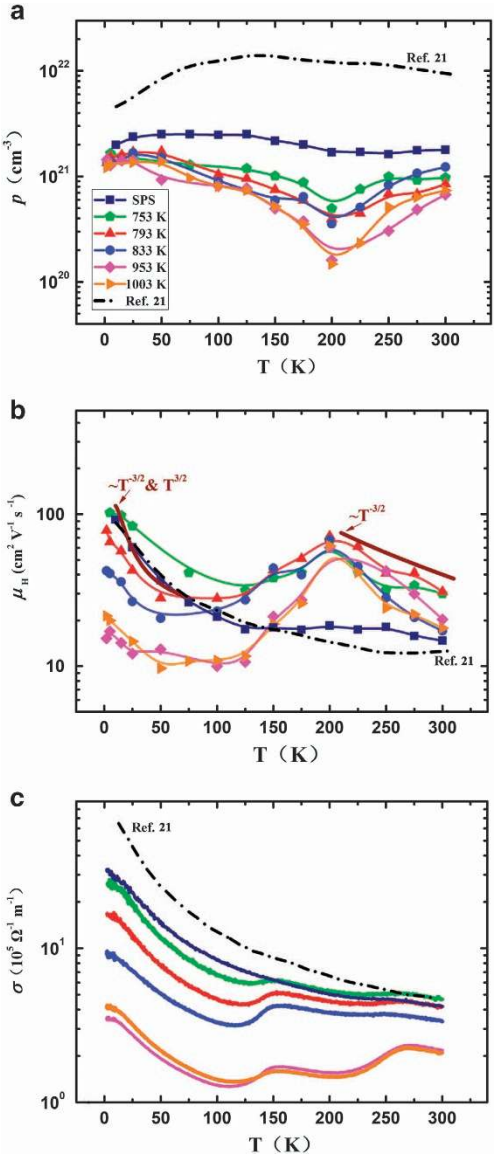

Figure 5 Temperature dependence of the carrier transport properties at low temperatures. (**a**) Carrier concentrations (p), (**b**) carrier mobility (μ_H) and (**c**) electrical conductivity (σ).

than Cu_2S and Cu_2Se, it is less ionic, which is typically a dominating factor in determining carrier mobility. As indicated in Supplementary Figure S4, the mobility in Cu_2Te is much larger than that in Cu_2S and similar to that in Cu_2Se.

We used a single parabolic band model with the carrier scattering limited by phonons above the ambient temperature to analyze the electronic properties of our samples. We assumed the carrier concentrations would not change much at high temperatures owing to the degenerately doped sample. The thermopower as a function of carrier concentration at 300 K is shown in Figure 6a. All the samples had good agreement with the Pisarenko relation at 300 K with m^*/m_0 equal to approximately 1.7. Note that the m^*/m_0 value in Cu_2Te was similar to those in Cu_2S and Cu_2Se,[16] but its carrier concentration was 1–3 orders higher than those of Cu_2S and Cu_2Se. This indicates that there was no clear alteration in the band structure among the samples using different process treatments, and the electrical transports were determined primarily by the carrier concentrations in our Cu_2Te samples. The room-temperature mobility as a function of carrier concentration is also plotted in Figure 6b. The figure shows a reduced trend as carrier concentration increased and reveals a relationship of $\mu_H \propto p^{-1/3}$, which accords with the common electron-phonon interaction. Additionally, we attempted to determine the optimal carrier concentration to obtain the best electrical properties. The *PF* as a function of carrier concentration for both the experimental data and the simulated results based on the single parabolic band model at 300 and 900 K is shown in Figure 6c. Apparently, the optimal carrier concentration in Cu_2Te is approximately $7–9 \times 10^{19}\,cm^{-3}$ at 300 K and $2–4 \times 10^{20}\,cm^{-3}$ at 1000 K. This indicates that the carrier concentrations in both the referenced samples and our samples were too high. This explains, in part, why the reported zTs in $Cu_{2-\delta}Te$ were lower than those in $Cu_{2-\delta}Se$ and $Cu_{2-\delta}S$. Nevertheless, the Cu_2Te samples using direct annealing had greatly reduced carrier concentrations, approaching the optimal values, as compared with the samples using SPS. This explains the observed enhanced *PF*s shown in Figure 4.

The enhancement in zT in our directly annealed samples was caused not only by the optimization of the carrier concentrations but also by the substantially reduced carrier thermal conductivity as well as the total thermal conductivity. Cu_2S and Cu_2Se have extremely low lattice thermal conductivity. Therefore, Cu_2Te is also expected to possess a much lower lattice thermal conductivity when considering the character of the heavy element Te as well as the complicated crystal structure. However, as shown in Figure 3c, Cu_2Te had a relatively high total thermal conductivity, above $2\,W\,m^{-1}\,K^{-1}$, at room temperature. By considering its very high electrical conductivity, it is likely that the charge carriers dominated the total thermal conductivity. Therefore, large errors can occur when estimating the separated contributions to the total thermal conductivity from the lattice phonons and charge carriers as well as the additional, very small deviation in the transports in different directions (see Supplementary Figure S2). If we assume κ_L is $0.2\,W\,m^{-1}\,K^{-1}$, the estimated Lorenz number using the Wiedemann-Franz law is between 1.0 and 1.6 $10^{-8}\,V^2\,K^{-2}$ (see Supplementary Figure S5). The electronic contribution is more than 80–90%. Nevertheless, the extremely large contribution to the thermal conductivity from the charge carriers suggests that the optimization of the TE properties in Cu_2Te must also considerably reduce κ_c. As shown in Figure 5a, the reduced carrier concentrations in the directly annealed Cu_2Te samples not only tuned *PF*s to approach the optimal value but also significantly lowered the κ_c as well as the total thermal conductivity. Thus, combining these two effects significantly improved the zT from 0.55 to 1.1 (see Figure 3d).

$Cu_{2-x}Te$ has too many carriers, which is due primarily to the easy formation of defects, such as the Cu vacancy. The observed lowered carrier concentration in the directly annealed Cu_2Te is interesting and nonintuitive. In general, formation of the donor defects, such as the Te vacancy (V_{Te}) or the Cu interstitial (Cu_i), can lower the hole carrier density in the system. The normal SPS process is performed in a vacuum; thus, the element Te could have evaporated. The formation of V_{Te} could reduce the copper deficiencies, resulting in low carrier concentrations. However, the observed high carrier concentration in the SPS-Cu_2Te samples indicates that this was not the case, suggesting that the observed behavior is not a surface-induced effect. After analyzing the experimental processes and theoretical analysis, we believe that the observed phenomena can be explained as follows. The directly annealed Cu_2Te samples undergo a long and slow thermal annealing process to reach thermal equilibrium; thus, the charge-compensating defects, such as Cu and Te vacancies, can reach thermal equilibrium concentration, which results in lower carrier densities. By

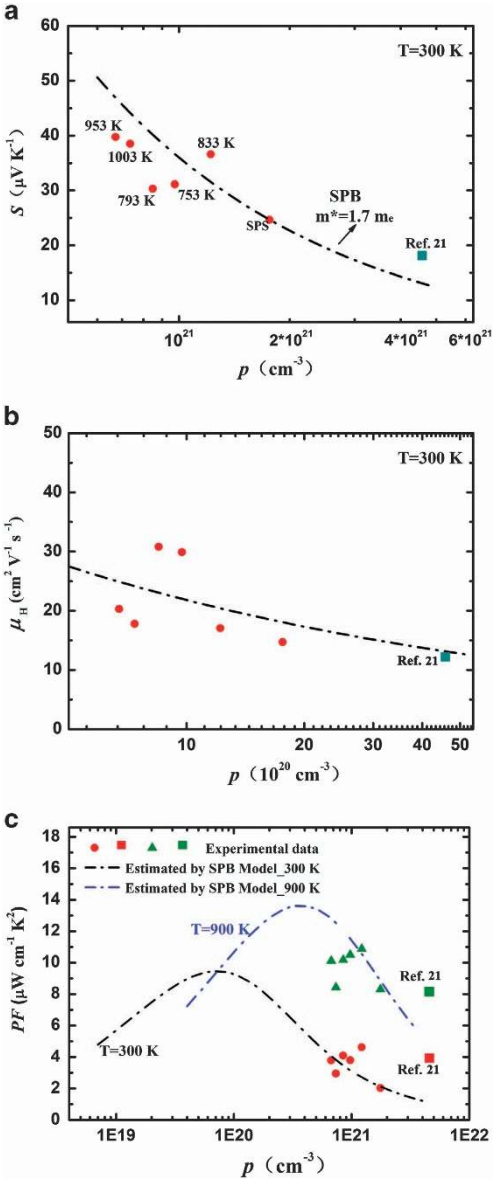

Figure 6 (**a**) Thermopower (*S*) as a function of the carrier concentration, (**b**) carrier mobility (μ_H) as a function of the carrier concentration and (**c**) power factor (*PF*) as a function of carrier concentration. The dashed dot lines are simulated by a single parabolic band model (SPB).

contrast, during the SPS process, rapid heating and cooling processes lead to nonequilibrium growth, which can enhance the formation of the dominant defect (V_{Cu}) and suppress the compensating one (V_{Te}) because the charged defect formation energy is a function of the Fermi energy, and at high growth temperatures, the Fermi energy could be pinned by the band edge excitation. After rapid nonequilibrium cooling from high temperature, the remaining intrinsic defects can dominate over the band-to-band thermal excitations and other types of defects, which will shift the Fermi energy to the valance band and achieve a higher carrier concentration.[31] Moreover, in the direct annealing process, the sample is sealed in the tube, which is a closed system without any additional factors to affect the materials, except the temperatures; thus, the chemical compositions in the directly annealed samples should be closer to the designed values. At a high annealing temperature, Cu_i may easily form, which can also reduce the hole carrier density. Moreover, omission of the sintering process and instead using SPS for obtaining high-density Cu_2Te samples simplifies the synthesis process and improves the sample's TE properties. Therefore, it is easy to obtain samples with compositions equal to the designed values. It is important to achieve high TE performance and other physical properties in semiconducting materials.

CONCLUSIONS

In summary, we used the normal SPS process to study the TE properties of Cu_2Te bulk materials. Very high electrical and thermal conductivity were observed, which led to low *zT* values. We then omitted the SPS process and used a direct annealing procedure to synthesize Cu_2Te bulk samples. Surprisingly, very high density was obtained in the directly annealed samples, with values similar to those for the samples generated using SPS. The crystal structures in the directly annealed samples were complicated because they were influenced by the heat treatment processes. The carrier concentrations in the directly annealed samples were much lower than that in the SPS sample, leading to reduced electrical conductivity and greatly enhanced thermopower. A single parabolic band model was used to analyze the electrical transports. The lowered carrier concentrations in the directly annealed samples were close to the optimal value, which resulted in optimized electrical transports with large *PF*s. In addition, the total thermal conductivity was significantly reduced because of the greatly reduced contributions from the charge carriers. These two favorable factors led to the *zT* values being significantly improved, from 0.55 in the SPS sample to 1.1 in the directly annealed samples at 1000 K. The current study, as well as those of $Cu_{2-\delta}Se$ and $Cu_{2-\delta}S$, demonstrates that $Cu_{2-\delta}X$ (X = S, Se and Te) is the only material system to show high *zT* values in the series of compounds composed of three sequential primary group elements.

CONFLICT OF INTEREST

The authors declare no conflict of interest.

ACKNOWLEDGEMENTS

This work is supported by the National Basic Research Program of China (973 program) under project no. 2013CB632501, the National Natural Science Foundation of China (NSFC) under nos. 51472262 and 51222209, the Key Research Program of Chinese Academy of Sciences (grant no. KGZD-EW-T06) and the Shanghai government (grant no. 14DZ2261200 and no. 15JC1400301).

1 Bell, L. E. Cooling, heating, generating power, and recovering waste heat with thermoelectric systems. *Science* **321**, 1457–1461 (2008).
2 Ioffe, A. F. *Semiconductor Thermoelements and Thermoelectric Cooling*, (Infosearch Limited, London, 1957).
3 Snyder, G. J. & Toberer, E. S. Complex thermoelectric materials. *Nat. Mater.* **7**, 105–114 (2008).
4 Shi, X., Yang, J., Salvador, J. R., Chi, M. F., Cho, J. Y., Wang, H., Bai, S. Q., Yang, J. H., Zhang, W. Q. & Chen, L. D. Multiple-filled skutterudites: high thermoelectric figure of merit through separately optimizing electrical and thermal transports. *J. Am. Chem. Soc.* **133**, 7837–7846 (2011).
5 Heremans, J. P., Jovovic, V., Toberer, E. S., Saramat, A., Kurosaki, K., Charoenphakdee, A., Yamanaka, S. & Snyder, G. J. Enhancement of thermoelectric efficiency in PbTe by distortion of the electronic density of states. *Science* **321**, 554–557 (2008).
6 Lan, J. L. Y., Liu, C., Zhan, B., Lin, Y. H., Zhang, B. P., Yuan, X., Zhang, W. Q., Xu, W. & Nan, C. W. Enhanced thermoelectric properties of Pb-doped BiCuSeO ceramics. *Adv. Mater.* **25**, 5086–5090 (2013).
7 Hsu, K. F., Loo, S., Guo, F., Chen, W., Dyck, J. S., Uher, C., Hogan, T., Polychroniadis, E. K. & Kanatzidis, M. G. Cubic AgPbmSbTe2+m: bulk thermoelectric materials with high figure of merit. *Science* **303**, 818–821 (2004).
8 Liu, W., Tan, X. J., Yin, K., Liu, H. J., Tang, X. F., Shi, J., Zhang, Q. J. & Uher, C. Convergence of conduction bands as a means of enhancing thermoelectric performance of n-type Mg2Si(1-x)Sn(x) solid solutions. *Phys. Rev. Lett.* **108**, 166601 (2012).

9 Fu, C. G., Zhu, T. J., Pei, Y. Z., Xie, H. H., Wang, H., Snyder, G. J., Liu, Y., Liu, Y. T. & Zhao, X. B. High band degeneracy contributes to high thermoelectric performance in p-type half-heusler compounds. *Adv. Energy Mater* **4**, 1400600 (2014).
10 Zhao, H. Z., Sui, J. H., Tang, Z. J., Lan, Y. C., Jie, Q., Kraemer, D., McEnaney, K., Guloy, A., Chen, G. & Ren, Z. F. High thermoelectric performance of MgAgSb-based materials. *Nano Energy* **7**, 97–103 (2014).
11 Liu, H. L., Shi, X., Xu, F. F., Zhang, L. L., Zhang, W. Q., Chen, L. D., Li, Q., Uher, C., Day, T. & Snyder, G. J. Copper ion in liquid-like thermoelectrics. *Nat. Mater.* **11**, 422–425 (2012).
12 Yu, B., Liu, W. S., Chen, S., Wang, H., Wang, H. Z., Chen, G. & Ren, Z. F. Thermoelectric properties of copper selenide with ordered selenium layer and disordered copper layer. *Nano Energy* **1**, 472–478 (2012).
13 Liu, H. L., Yuan, X., Lu, P., Shi, X., Xu, F. F., He, Y., Tang, Y. S., Bai, S. Q., Zhang, W. Q., Chen, L. D., Lin, Y., Shi, L., Lin, H., Gao, X.Y., Zhang, X. M., Chi, H. & Uher, C. Ultrahigh thermoelectric performance by electron and phonon critical scattering in Cu2Se1-xIx. *Adv. Mater.* **25**, 6607–6612 (2013).
14 Liu, H. L., Shi, X., Kirkham, M., Wang, H., Li, Q., Uher, C., Zhang, W. Q. & Chen, L. D. Structure-transformation-induced abnormal thermoelectric properties in semiconductor copper selenide. *Mater. Lett.* **93**, 121–124 (2013).
15 Su, X. L., Fu, F., Yan, Y. G., Zheng, G., Liang, T., Zhang, Q., Cheng, X., Yang, D. W., Chi, H., Tang, X. F., Zhang, Q. J. & Uher, C. Self-propagating high-temperature synthesis for compound thermoelectrics and new criterion for combustion processing. *Nat. Commun* **5**, 4908 (2014).
16 He, Y., Day, T., Zhang, T. S., Liu, H. L., Shi, X., Chen, L. D & Snyder, G. J. High thermoelectric performance in non-toxic earth-abundant copper sulfide. *Adv. Mater.* **26**, 3974–3978 (2014).
17 Ge, Z. H., Zhang, B. P., Chen, Y. X., Yu, Z. X., Liu, Y. & Li, J. F. Synthesis and transport property of Cu(1.8)S as a promising thermoelectric compound. *Chem. Commun.* **47**, 12697–12699 (2011).
18 Mehta, R. J., Zhang, Y. L., Karthik, C., Singh, B., Siegel, R. W., Tasciuc, T. B. & Ramanath, G. A new class of doped nanobulk high-figure-of-merit thermoelectrics by scalable bottom-up assembly. *Nat. Mater.* **11**, 233–240 (2012).
19 Tang, X. F., Xie, W. J., Li, H., Zhao, W. Y., Zhang, Q. J. & Niino, M. Preparation and thermoelectric transport properties of high-performance p-type Bi2Te3 with layered nanostructure. *Appl. Phys. Lett.* **90**, 012102 (2007).
20 Du, B. L., Li, H., Xu, J. J., Tang, X. F. & Uher, C. Enhanced figure-of-merit in Se-doped p-type AgSbTe2 thermoelectric compound. *Chem. Mater.* **22**, 5521–5527 (2010).
21 Ballikaya, S., Chi, H., Salvadorc, J. R. & Uher, C. Thermoelectric properties of Ag-doped Cu2Se and Cu2Te. *J. Mater. Chem. A* **1**, 12478 (2013).
22 Kurosaki, K., Kosuga, A., Muta, H. & Yamanaka, S. Thermoelectric and thermophysical characteristics of Cu2Te-TI2Te pseudo binary system. *Mater. Trans.* **47**, 1432–1435 (2006).
23 Zhao, L. D., Dravidb, V. P. & Kanatzidis, M. G. The panoscopic approach to high performance thermoelectrics. Energy Environ. *Sci.* **7**, 251–268 (2014).
24 Nowotny, H. Die Kristallstruktur von Cu2Te, *Z. Metallkd.* **37**, 40–42 (1946).
25 Asadov, Y. G., Rustamova, L. V., Gasimov, G. B., Jafarov, K. M. & Babajev, A. G. Structural phase transitions in Cu2-xTe crystals (x=0.00, 0.10, 0.15, 0.20, 0.25). *Phase Transitions* **38**, 247–259 (1992).
26 Lin, H., Chen, H., Shen, J. N., Chen, L. & Wu, L. M. Chemical modification and energetically favorable atomic disorder of a layered thermoelectric material TmCuTe2 leading to high performance. *Chemistry* **20**, 15401–15408 (2014).
27 Kashida, S., Shimosaka, W., Mori, M. & Yoshimura, D. Valence band photoemission study of the copper chalcogenide compounds, Cu2S, Cu2Se and Cu2Te. *J. Phys. Chem. Solids* **64**, 2357–2363 (2003).
28 Zhang, Y. G., Sa, B. S., Zhou, J. & Sun, Z. M. First principles investigation of the structure and electronic properties of Cu2Te. *Comput. Mater. Sci.* **81**, 163–169 (2014).
29 Juarez, L. F., Silva, D., Wei, S. H., Zhou, J. & Wu, X. Z. Stability and electronic structures of CuxTe. *Appl. Phys. Lett.* **91**, 091902 (2007).
30 Bougnot, J., Guastavino, F., Luquet, H. & Sodini, D. Study of region of existence of alpha phase of copper tellurium using electric conductivity. *Mater. Res. Bull.* **5**, 763–767 (1970).
31 Yang, J. H., Park, J. S., Kang, J., Metzger, W., Barnes, T. & Wei, S. H. Tuning the Fermi level beyond the equilibrium doping limit through quenching: The case of CdTe. *Phys. Rev. B* **90**, 245202 (2014).

Supplementary Information accompanies the paper on the NPG Asia Materials website (http://www.nature.com/am)